Mol Cell Toxicol (2019) 15:255-264
DOI 10.1007/s13273-019-0029-5

ORIGINAL PAPER

Transcriptomics and proteomics analysis of Aβ (1-42)-induced neurotoxicity

Zhonghao Su[1], Zhuo Dong[2], Chunxia Guo[1], Ying Xu[1], Shuijin Shao[1] & Zhenxia Qin[1]

Received: 12 September 2018 / Accepted: 31 January 2019

Abstract

Backgrounds: β-Amyloid (Aβ) is a principal constituent of senile plaques in Alzheimer's disease (AD) and induces neuronal cell death. The molecular mechanism of how Aβ evokes neuronal cell death remains complicated, which were investigated in the present study.
Methods: Using the human neuroblastoma cell line SH-SY5Y, we investigated the neurotoxic effects of human β-Amyloid 1-42 ($A\beta_{1-42}$) aggregates on gene expression profile and protein expression profile by using the Agilent GeneChip Human 1A (V2) Oligo MicroArray, Quantitative Real-time PCR, PF-2D and Western blot analysis.
Results: Our results show that $A\beta_{1-42}$ specifically influences gene and protein expression such as EGR1, eIF5A, PDE8A, ERp57 and ERp5 in pathways associated with apoptotic process, protein translation, cAMP catabolic process and response to endoplasmic reticulum stress.
Conclusion: Although Genes with significant changes in transcriptomic analysis matched very few of the proteins identified in proteomics analysis, our findings will strengthen our knowledge concerning the molecular mechanisms underlying AD.

Keywords: β-Amyloid peptide, Neurotoxicity, Neuroblastoma cells, Microarray, PF-2D

[1]School of Basic Medicine, Shanghai University of Traditional Chinese Medicine, Shanghai 201203, China
[2]Shanghai Key Laboratory of Brain Functional Genomics, Ministry of Education, East China Normal University, Shanghai 200062, China
Correspondence and requests for materials should be addressed to
Z. X. Qin (✉zhenxiaq@163.com) &
S. J. Shao (✉13917183283@163.com)

Introduction

The hallmark pathologies of Alzheimer's disease (AD) are the presence of amyloid-beta peptide (Aβ) deposition, neurofibrillary tangle (NFT) formation as well as neuronal loss. Several studies suggest that Aβ may play a crucial role in the pathogenesis of AD in vitro and in vivo[1-4]. Despite several years of intense research, the exact molecular mechanism of Aβ-caused neurotoxicity had not been definitely identified.

The genes differentially expressed have been identified in the neurotoxic model of Aβ using a cDNA microarray[5-7]. However, no conformities were achieved among these researches, the differences could be derived from the use of the neuronal model and different arrays platforms in these studies. The data obtained by proteomic analysis should enrich the information generated by microarray-studies, as there is a lack of correlation between transcriptional profiles and actual protein levels in many studies[8,9]. The ProteomeLab PF-2D platform (Beckman Coulter, Fullerton, CA) can be used for chromatofocusing separation, hydrophobic fractionation and comparing various biological samples quantitatively. Compared to gel-based 2-DE, the PF-2D system possess good reproducibility, high loading capacity, and improved detection of lower abundance proteins[10].

In the present study, differential proteomic analysis with a two-dimensional (2D) liquid chromatography-based proteomic approach (PF-2D system) and gene expression profiling analysis based on cDNA microarray were used to identify the differentially expressed genes and proteins in SH-SY5Y cells treated by $A\beta_{1-42}$. The findings were subsequently confirmed in an independent group of $A\beta_{1-42}$-treated cells and mock-cells by real-time PCR and Western bolt analysis. The study may provide more molecular targets that allow for un-

Table 1. The primers used for Quantitative Real-time PCR.

Gene name	Forward primer	Reverse primer
GRIN2B	5′-GAAGAACTGGAAGCTCTCTGGC-3′	5′-GAAGAACTGGAAGCTCTCTGGC-3′
TRAF1	5′-GTGTCGGCTGCTCCTTCAA-3′	5′-CAAACACACGCAGCTTCCC-3′
PDE4C	5′-CAAGTTCAAGCGGATCCTGAAC-3′	5′-GCCACCTTGAACACATCAAGTC-3′
GRP58	5′-CATTTTTGGTATCTGCCCTCACA-3′	5′-AACTCCTCCTGCATGACAAACTTC-3′
TCF7	5′-GACCGCAACCTGAAGACACA-3′	5′-GACCGCCTCTTCTTCTTCCC-3′
EGR1	5′-AGCAGCACCTTCAACCCTCA-3′	5′-TCATGCTCACTAGGCCACTGAC-3′
β-actin	5′-GGACATCCGCAAAGACCTGTA-3′	5′-ACATCTGCTGGAAGGTGGACA-3′

derstanding the mechanisms of $A\beta_{1\text{-}42}$-induced neurotoxicity in AD.

Materials & Methods

Cell culture and treatments

SH-SY5Y human neuroblastoma cells were obtained from ATCC and cultured as previously described[11]. Synthetic $A\beta_{1\text{-}42}$, obtained from CPC Scientific Inc, was dissolved in distilled water at a concentration of 1 mM and stored at −20°C. Previous to the experiments the stock solution was diluted to the desired concentrations, maintained for 3d at 37°C to form aggregation and then added to the culture medium. SH-SY5Y cells (1×10^5) were mocked or treated with 10 μM $A\beta_{1\text{-}42}$ in Opti-MEM I medium for 24 h in a 6-well plate, then the cells were collected for microarray, real-time PCR, PF-2D analysis and Western blot analysis.

Gene microarray analysis

Total RNA was isolated from human SH-SY5Y cells according to manufacturer's recommendations (Trizol, Invitrogen). Quantification of RNA was performed with spectrophotometry (ND-1000; NanoDrop Products, Thermo Fisher Scientific, Wilmington, DE). Total RNA integrity was determined with a bioanalyzer (model 2100; Agilent Technologies, Palo Alto, CA) according to the manufacturer's protocol. Agilent GeneChip Human 1A (V2) Oligo Microarray (Agilent Technologies, USA) was used to analyze the gene expression profile in SH-SY5Y cells. This microarray contains 22,575 well-characterized human genes. Preparation of cDNA, cRNA, hybridization and scanning of microarrays were performed following manufacturer's protocols (Agilent Technologies). The fluorescent labeled cRNA was prepared for oligo microarray hybridization. cRNA from SH-SY5Y cells without or with $A\beta_{1\text{-}42}$ treatment was labled with Cy3- or Cy5-CTP, respectively. Each experiment was repeated twice with a switch of fluorescent Cy3/Cy5 labels to exclude dye effects. Washing, staining, and scanning were performed by using the Genechip Instrument System (Agilent) as recommended in the manufacturer's technical manual. Microarray scanner system (Agilent, USA) was used for data analysis. The ratio between Cy5 processed signal and Cy3 processed signal after feature extraction by Feature Extraction software were calculated as log ratio values and converted to fold change (FC). Those genes with more than 1.5-fold change in all four comparisons were considered for additional verification.

Quantitative real-time PCR

Some of the genes identified from microarray experiment were validated by fluorescence real-time quantitative RT-PCR. cDNA was generated from the total RNA samples identical with the ones used for the chip analysis (Taqman reverse transcription reagents kit). The primers in Table 1 were designed using Primerexpress software and synthesized by Invitrogen. β-actin was used as a reference gene. PCR amplification was performed with master mix (TaqMan Universal PCR Master Mix with Bio-rad). All PCR reactions were performed in triplicate. The experiment was performed on the Opticon 2 (MJ research, USA). The relative quantification was used to analyze the differential expression of genes. Gene expression levels were calculated and presented with $2^{-\Delta\Delta Ct}$values.

PF-2D analysis

The cell lysates from $A\beta_{1\text{-}42}$-treated and mock-treatment cells were obtained by using lysis buffer (6 M urea, 2 M thiourea, 10% glycerol, 50 mM Tris-HCl (pH 7.8-8.2), 2% n-OG, 1 mM protease inhibitor) at room temperature for 30 min to ensure proper denaturation in three independent biological replicates. Ultrasonic treatment 20 s each time with a 10 s interval for the lysates on ice was performed 3 times to avoid nucleotides contamination. The lysates were centrifuged at 18°C at 20,000 ×g for 60 min. The supernatants were removed and stored at −70°C. All buffers and columns were purchased from Beckman Coulter, and the ProteomeLab PF-2D system (Beckman Coulter) was used for the entire analysis. Protein concentrations were measured

by the BCA assay and adjusted to a concentration of 2 mg/mL with first dimension starting buffer.

A high-performance chromatofocusing (HPCF) column was used to perform the first-dimension chromatofocusing under ambient temperature at a flow rate of 0.2 mL/min. Before each run, the column was equilibrated with starting buffer (pH 8.5). Twenty minutes after the sample injection, protein peaks in the elution buffer (pH 4.0) were monitored by absorbance at 280 nm. The first-dimension fractions were collected into 96-well plates at a pH interval of 0.3.

The second dimension separations were performed using a Beckman Coulter nonporous reverse phase (NPRP) column at 55°C. The column was first equilibrated with solvent A (0.1% (v/v) aqueous trifluoroacetic acid (TFA)) for 8 min before sample injection. Aliquots of 0.2 mL of each chromatofocusing fraction were resolved for two minutes and followed by elution with 0-100% gradient of solvent B (0.08% (v/v) TFA in acetonitrile) for 30 min and 100% solvent B for 4 min. Re-equilibration was achieved with 100% solvent A. Proteins fractions were separated at a flow rate of 0.75 mL/min and monitored by UV absorbance at 214 nm. The second-dimension fractions were collected in 96-well plates at a rate of 0.25 min/well using a FC204 fraction collector (Gulson, France) and stored at −70°C.

During PF-2D operation, protein peaks were analyzed with 32 Karat software. The proteome profile from second-dimension chromatographies was imported into ProteoVue and DeltaVue programs for the final analysis. Fractions with more than 2 or less than 0.5-fold change in the expression were considered significant and subjected to the subsequent MALDI-TOF/TOF analysis.

Protein identification by MALDI-TOF/TOF mass spectrometry

All fractions from the second dimension were lyophilized and stored at −70°C before digestion. The fractions were redissolved in 25 mM NH_4HCO_3 buffer and reduced by boiling for 1 min. Proteins were digested overnight at 37°C with trypsin at a mass ratio of 50 : 1. Tryptic peptides were mixed with 1 μL of matrix solution of α-cyano-4-hydroxycinnamic acid (CHCA) in 50% (v/v) acetonitrile (ACN) and 0.1% (v/v) TFA in water, spotted to the MALDI plate. The measurements were acquired in positive mode on an ABI 4700 Proteomics Discovery System (Applied Biosystems, USA). The interpretation of PMF data with S/N above 20 and MS/MS data with S/N above 5 were carried out with the GPS Explore software 3.6 (Applied Biosystems, USA) based on MASCOT search engine. Protein identifications with score greater than 64 or the best ion score (MS/MS) over 34 were positively assigned.

Western blot analysis

The harvested cells were homogenized with lysis buffer (Beyotime, Jiangsu, China). Protein concentration was measured with BCA assay. Equal amount of protein (20 μg) from each sample was boiled for 5 min in loading buffer (5% mercaptoethanol, 0.05% bromphenol blue, 75 mmol/L Tris-HCl, pH 6.8, 2% SDS, and 10% glycerol). Proteins were resolved by 7.5% SDS-PAGE gel and transferred to PVDF membranes (Millipore, MA, USA) using the Wet/Tank Blotting System (BioRad, CA, USA). After being blocked with 5% nonfat dried milk in 1×TBS-T buffer (20 mmol/L Tris-HCl, pH 7.5, 137 mmol/L NaCl and 0.05% Tween-20) for 1 h at room temperature, membranes were incubated with primary antibodies including rabbit anti-H2A, rabbit anti-eIF5A and rabbit anti-β-actin (Cell Signaling Technology, MA, USA) at a 1 : 8000 dilution in 1×TBS-T buffer at 4°C overnight. The blots were washed and incubated with anti-rabbit secondary antibodies (1 : 10000) for 1 h at room temperature. Chemiluminescent detection was performed using an ECL Western blotting Detection kit from Amersham Pharmacia (Buckinghamshire, UK).

Functional enrichment analysis

In the GO analysis, the categories of differentially expressed genes (DEGs) including cellular component (CC), biological process (BP) and molecular function (MF) terms were analyzed using the Biological Processes and Molecular Functions Enrichment Analysis Database for Annotation, Visualization and Integrated Discovery (DAVID) (http://david.abcc.ncifcrf.gov/). P value <0.05 was regarded as statistically significant differences.

Statistical analysis

Data were calculated as the mean ± SEM by Sigmaplot 9.0 (Systat Software Inc, USA). Statistical significances were determined by student's t-test and shown as $*P<0.05$, $**P<0.01$ and $***P<0.001$.

Results

Global transcriptional response to $A\beta_{1\text{-}42}$ stimulation

We previously determined that $A\beta_{1\text{-}42}$-induced apoptosis in human neuroblastma cell line SH-SY5Y[3,11]. To further elucidate the molecular mechanism of $A\beta_{1\text{-}42}$-induced neurotoxicity, based on prior works in our laboratory, we investigated the effect of $A\beta_{1\text{-}42}$ treatment

Table 2. $A\beta_{1-42}$-increased genes.

Gene name	Access number	Fold increase
CGI-116 protein (CGI-116)	NM_016053	17.38
Laminin, beta 1 (LAMB1)	NM_002291	7.64
Muscleblind-like 2 (Drosophila) (MBNL2)	NM_144778	4.95
Killer cell lectin-like receptor subfamily B, member 1 (KLRB1)	NM_002258	3.74
Phosphodiesterase 8A (PDE8A)	NM_002605	3.55
SAM pointed domain containing ets transcription factor (SPDEF)	NM_012391	2.97
Solute carrier family 39 (metal ion transporter), member 5 (SLC39A5)	AK313188	2.85
Histone 2, H2ac (HIST2H2AC)	NM_003517	2.74
Sperm associated antigen 16	BC067756	2.66
Osteoglycin (osteoinductive factor, mimecan) (OGN)	NM_033014	2.52
Hypothetical protein FLJ13639	NM_024705	2.42
cDNA FLJ13769 fis, clone PLACE4000222	AK023831	2.24
WD repeat domain 48 (WDR48)	NM_020839	2.17
PIF1 5′-to-3′ DNA helicase homolog (S. cerevisiae)	NM_025049	2.1
RAD54 homolog B (S. cerevisiae) (RAD54B)	NM_012415	2.04
cDNA FLJ46355 fis, clone TESTI4049110	AK128222	1.99
Early growth response 1 (EGR1)	NM_001964	1.85
KCNH2	NM_172056	1.72
C20orf196	NM_152504	1.63
Sjogren's syndrome/scleroderma autoantigen 1 (SSSCA1)	NM_006396	1.6
Prefoldin 2 (PFDN2)	NM_012394	1.57
Heterogeneous nuclear ribonucleoprotein A0 (HNRPA0)	NM_006805	1.5
Glucose regulated protein, 58 kDa (GRP58/ERp57)	NM_005313	1.5
Kinesin family member C1, mRNA (cDNA clone IMAGE:3506669)	BC000712	1.5

Table 3. $A\beta_{1-42}$-decreased genes.

Gene name	Access number	Fold repression
Rad50-interacting protein 1 (RINT-1)	NM_021930	16.6
Solute carrier family 5 (iodide transporter), member 8 (SLC5A8)	NM_145913	4.78
Regulating synaptic membrane exocytosis 1 (RIMS1)	NM_014989	2.71
Glutamate receptor, ionotropic, N-methyl D-aspartate 2B (GRIN2B)	NM_000834	2.68
Transcription factor 7 (T-cell specific, HMG-box) (TCF7)	NM_003202	2.47
BRAF35/HDAC2 complex (80 kDa) (BHC80)	NM_016621	2.33
TNF receptor-associated factor 1 (TRAF1)	NM_005658	1.94
Phosphodiesterase 4C (PDE4C), transcript variant 1	NM_000923	1.8
LYG1	NM_174898	1.86
SPCX	AY168775	1.85
Class-I MHC-restricted T cell associated molecule (CRTAM)	NM_019604	1.84
Adrenomedullin receptor (ADMR/GPR182)	NM_007264	1.56
Cysteine and histidine-rich domain (CHORD)-containing, zinc binding protein 1 (CHORDC1)	NM_012124	1.56
Nucleotide binding protein-like (NUBPL)	NM_025152	1.56
Histone 1, H4i	BC016336	1.5

for 24 h on gene profile by performing microarray analysis with Agilent GeneChip Human 1A (V2) Oligo Microarray. For these experiments, mRNA samples isolated from cells exposed to $A\beta_{1-42}$ were compared to mRNA isolated from mock-treated cells. Overall, 39 genes showed a 1.5-fold or higher change in expression ($P \leq 0.05$). The 24 up-regulated genes and 15 down-regulated genes in $A\beta_{1-42}$-treated cells compared to mock-treated cells were shown in Table 2 and Table 3 respectively.

Among DEGs, some genes were validated by QPCR (Figure 1) using cDNA derived from total RNA of $A\beta_{1-42}$-treated cells and mock-treated cells. These included 2 genes that showed significant up-regulation by microarray and were confirmed with QPCR (EGR1 and GRP58). 4 genes investigated by QPCR were GRIN2B, PDE4C, TCF7 and TRAF1, which the microarray analysis indicated as down-regulated.

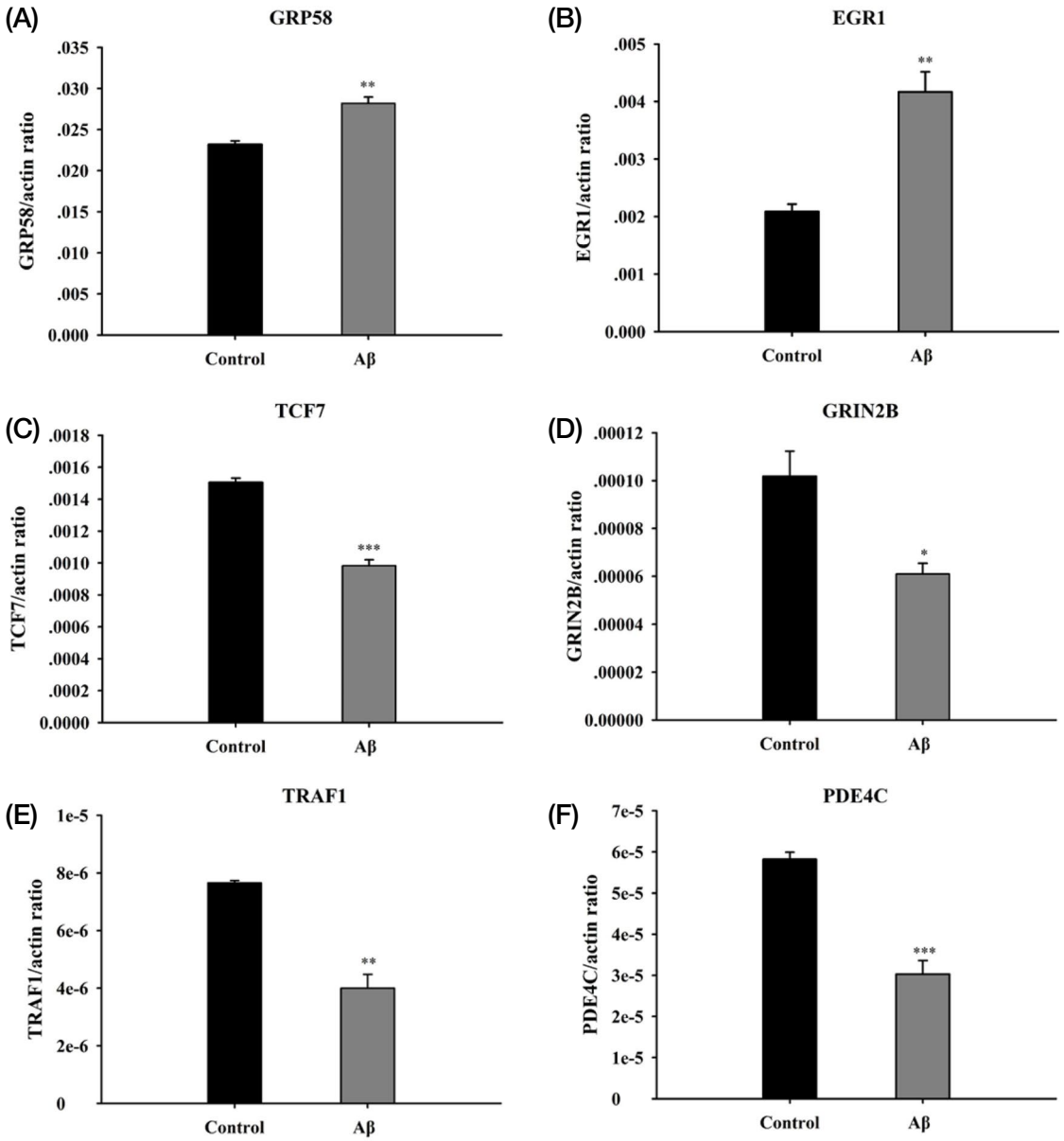

Figure 1. Validation of microarray data by quantitative real-time PCR. (A, B) GRP58 and EGR1 were increased significantly by $A\beta_{1\text{-}42}$ (10 μM) treatment for 24 h respectively. (C-F) TCF7, GRIN2B TRAF1 and PDE4C were decreased significantly by $A\beta_{1\text{-}42}$ (10 μM) treatment for 24 h respectively. Data are expressed as mean ± SEM from three independent experiments. Statistical significances were shown as $^{*}P<0.05$, $^{**}P<0.01$ and $^{***}P<0.001$.

Functional annotation and pathway enrichment

In order to shed light on the processes involved in $A\beta_{1\text{-}42}$ -induced neurotoxicity, enrichment of Gene Ontology (GO) terms among DEGs were analyzed in DAVID. Results for GO enrichment analysis are illustrated as Figure 2. In the CC ontology, we found that the majority of enriched categories were associated with nucleus (11 genes). In the BP ontology, the enriched categories comprised items related to DNA duplex unwinding (2 genes), cAMP catabolic process (2 genes) and beta-catenin-TCF complex assembly (2 genes). The zinc ion binding (4 genes), 3′,5′-cyclic-AMP phosphodiesterase activity (2 genes) and DNA helicase activity (2 genes) constitute the MF ontology.

Protein profiling of $A\beta_{1\text{-}42}$-induced neurotoxicity by PF-2D

We next examined the cell proteome profile of $A\beta_{1\text{-}42}$-

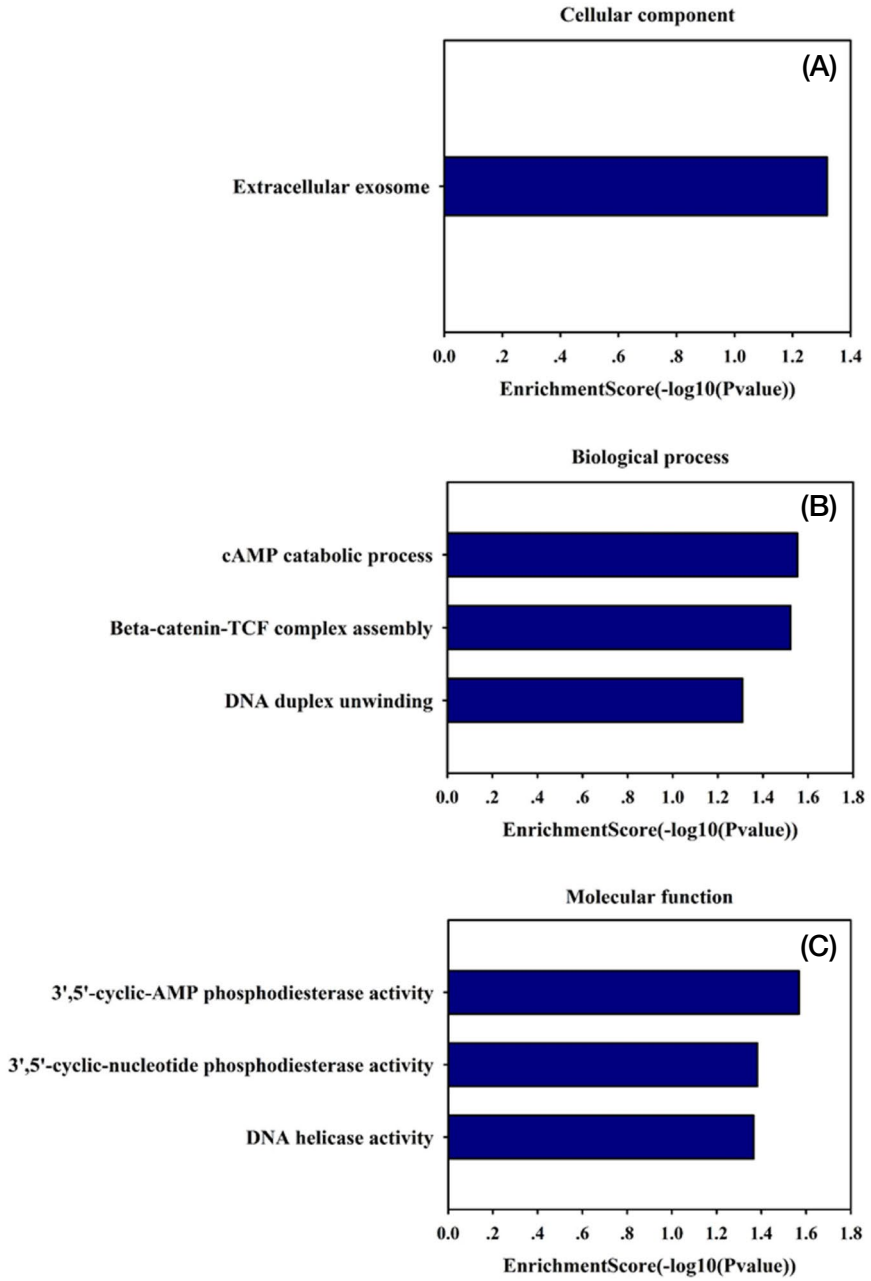

Figure 2. Go enrichment of DEGs by $A\beta_{1-42}$ in cellular component (A), biological process (B) and molecular function ontology (C).

stimulated neurotoxicity. It was hypothesized that such an examination could provide further insights into the neurotoxicity of $A\beta_{1-42}$. We used PF-2D system (Beckman, USA) to identify differentially expressed proteins associated with β-amyloid caused-neurotoxicity in SH-SY5Y cells. The first- and second-dimension separation of proteins based on their isoelectric points (pI) (Figure 3A) and hydrophobicity (Figure 3B) was shown in the virtual 2-D gel given by the software ProteoVue. In these experiments, 16 protein fractions were collected in the second dimension along the 8.5-4.5-pH gradient using the high performance reverse-phase chromatography. The 2D-maps from Control sample and $A\beta_{1-42}$-treated sample were compared and peak-to-peak analysis was performed by DeltaVue software to identify the differentially expressed proteins. Seventy-two peaks area ratio were beyond 2 including 34 up-regulated peaks and 38 down-regulated peaks and some peaks samples were selected for MS/MS analysis. A total of 13 proteins were identified by MS/MS

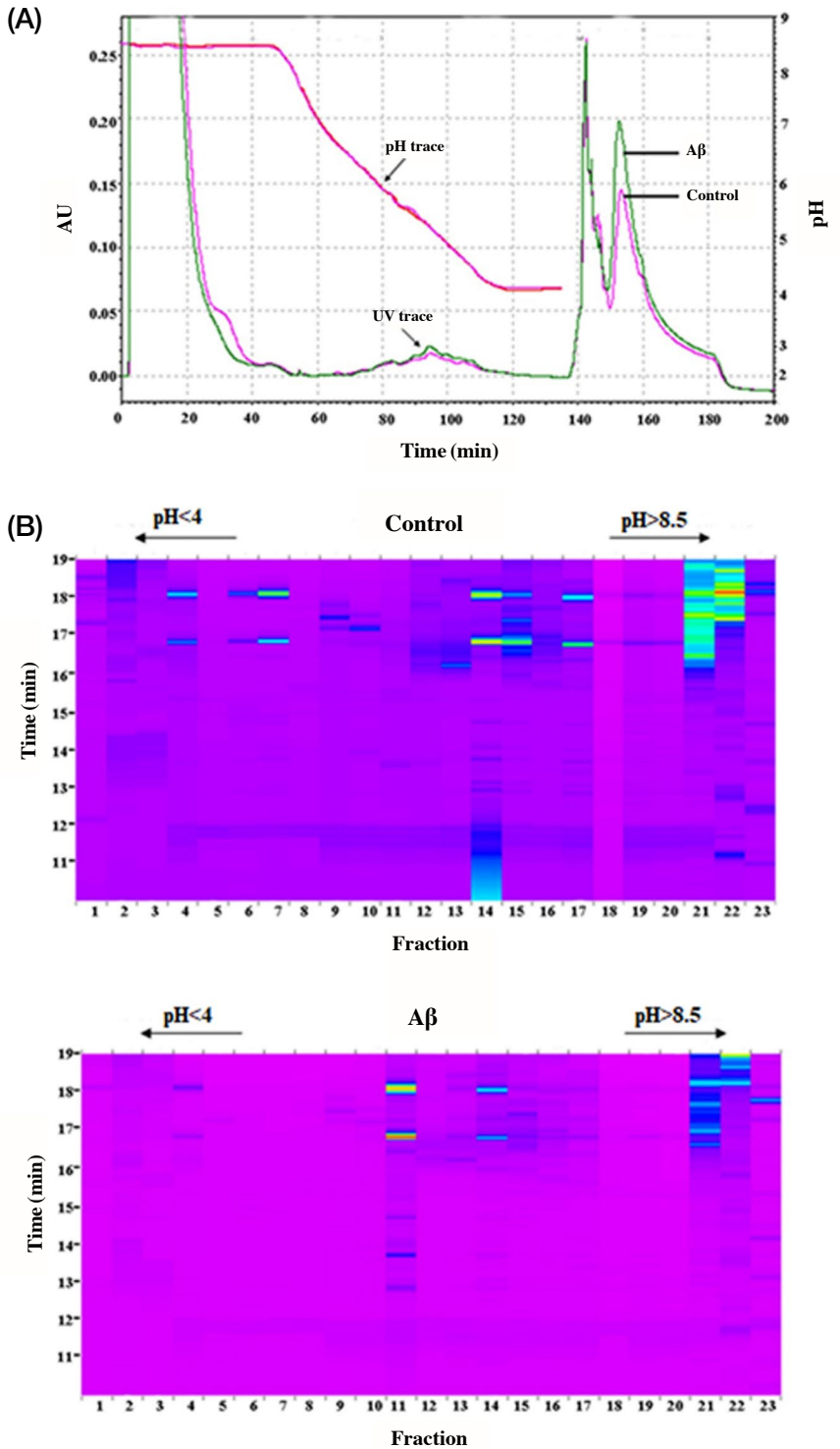

Figure 3. Chromatographic analysis of $A\beta_{1-42}$-treated and mock-treated cells proteins using ProteomeLab PF 2D. (A) Chromatofocusing of total proteins in a pH gradient. In the chromatogram, the X-axis corresponds to the retention time in the column, the left Y-axis to UV absorbance and the right Y-axis to the pH. (B) Resolution of ProteomeLab PF-2D in a virtual gel with Delta Vue software. Fractions are separated by pH gradient 8.5-4.0 and by hydrophobicity. The Y-axis corresponds to the column retention time in minutes, the upper X-axis indicates the pH gradients and the lower X-axis corresponds to the fraction number.

Table 4. Proteins separated by ProteomeLab PF-2D from cell lysates and identified by MALDI-TOF/MS.

Identified protein	gi accession #	pI/Mw (Da)	Score	Ratio
Histone H2A.2	gi|31979	10.21/ 13907.08	77	28.314 ↑
Unnamed protein product	gi|32113	10.11/ 13614.74	77	28.314 ↑
Histone H2B	gi|1568551	10.31/ 13936.17	77	28.314 ↑
H2B histone family, member A	gi|4504257	10.31/ 13906.14	77	28.314 ↑
H2B histone family, member C	gi|4504259	10.31/ 13952.21	77	28.314 ↑
H2B histone family, member D	gi|4504261	10.31/ 13922.14	77	28.314 ↑
H2B histone family, member E	gi|4504263	10.31/ 13989.27	77	28.314 ↑
H2B histone family, member J	gi|4504269	10.31/ 13892.11	77	28.314 ↑
H2B histone family, member Q	gi|4504277	10.31/ 13920.17	77	28.314 ↑
H2B histone family, member B	gi|10800138	10.31/ 13936.17	77	28.314 ↑
H2B histone family, member F	gi|10800140	10.31/ 13950.19	77	28.314 ↑
Protein Disulfide-isomerase A6 precursor (PDIA6/ERp5)	gi|62510933	4.95/ 46133.96	88	5.286 ↑
Eukaryotic translation initiation factor 5A (eIF5A)	gi|4503545	5.07/ 6832.25	80	3.229 ↓

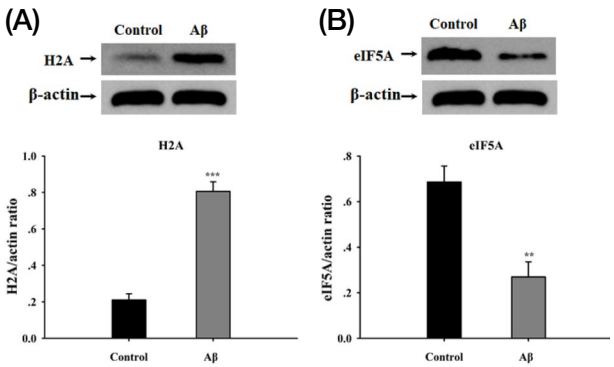

Figure 4. Detection of H2A and eIF5A by Western blotting analysis in Control group and Aβ group. (A) The expression of H2A was increased by $A\beta_{1\text{-}42}$ (10 μM) treatment for 24 h. (B) The expression of eIF5A mRNA was decreased by $A\beta_{1\text{-}42}$ (10 μM) treatment for 24 h. Data are expressed as mean ± SEM from three independent experiments. Statistical significances were shown as $^{***}P < 0.001$.

and NCBInr protein database (Table 4) which were involved in biological process: regulation of translation, chromatin silencing, response to endoplasmic reticulum stress, cell redox homeostasis and apoptosis.

To validate proteins identified by mass spectrometry, two proteins, H2A and eIF5A were detected by Western blot analysis with specific antibodies. The results showed that the mean levels of H2A were elevated by 3.8-fold (Figure 4A) and eIF5A were reduced by 2.5-fold (Figure 4B) in the $A\beta_{1\text{-}42}$-treated cells compared to those in Control cells. Trends of the changes were similar to those observed in the proteomic data.

Discussion

The human $A\beta_{1\text{-}42}$ peptide has been widely used as a valuable tool in vitro to analyze the pathogenic mechanisms that mediate AD. The neurotoxicity by $A\beta_{1\text{-}42}$ is under active investigation, which may occur in neurons of AD brain. Our results provided intriguing information on the molecular mechanism of Aβ-induced neurotoxicity.

In the present study, we investigated the global protein and gene profiles of SH-SY5Y cell line with $A\beta_{1\text{-}42}$ treatment using a PF-2D and microarray analysis, which enabled us to identify 52 differentially expressed proteins and genes between the $A\beta_{1\text{-}42}$ treated cell lines and control cell lines. Our lists of differentially regulated genes and differentially regulated proteins do not directly overlap except H2A protein. This is not only an issue for the current report but has been one for others who wish to complement microarray and proteomic studies[12]. It will be expected that more proteins identified by mass spectrometry, better parallel between changed genes and proteins. The differential expressions of proteins and genes were functionally related to biological process of cAMP catabolic process, regulation of immune response, mRNA processing, DNA repair, regulation of apoptotic process, protein folding, cell redox homeostasis, response to endoplasmic reticulum stress, regulation of ER to Golgi vesicle-mediated transport, synaptic vesicle exocytosis, learning or memory and others. The extensive protein and gene profile indicated that multiple cellular processes might be associated with $A\beta_{1\text{-}42}$-induced neurotoxicity.

Apoptosis is one of the fundamental mechanisms of cell death that occur during Aβ-caused neurotoxicity. As expected for the $A\beta_{1\text{-}42}$-treated cells, many of the apoptosis-related genes were differentially affected. It has been found that Early growth response 1 (Egr1) is elevated in AD brain[13]. Egr1 is a zinc finger transcription factor which regulates the transcription of a number of genes involved in apoptosis, immune response, cell proliferation, cell growth, and signal transduction. We also observed $A\beta_{1\text{-}42}$-induced apoptosis being ac-

companied by Egr1 induction.

Although the eukaryotic initiation factor 5A (eIF5A) was identified as the only known protein to contain the unusual amino acid, hypusine and originally proposed to stimulate protein synthesis initiation by transient binding to ribosomes, its actual function remains elusive. eIF5A mediates diverse intracellular functions such as cell growth including translation initiation, translation elongation[14], and the cell cycle[15] and cell death (apoptosis). Recent studies have also demonstrated a role for eIF5A as a regulator of apoptosis[16]. A very interesting result of our preliminary proteomic study is the identification of the decreased levels of eIF5A in $A\beta_{1-42}$-induced apoptosis, which indicates the involvement of eIF5 in the pathological mechanism of AD.

Consistent with previous reports[11], there was also a decrease in the expression of tumour necrosis factor receptor-associated factor 1 (TRAF1) in microarray studies after $A\beta_{1-42}$ treatment. TRAF1 exerts its diverse biological functions by associating with multiple receptors, kinases, adaptors and regulator proteins[17]. However, the role of TRAF1 in apoptosis remains undetermined. It have been shown that TRAF1 exerts both pro-apoptotic[18] and anti-apoptotic[19] effect during various types of stimuli. Our results may indicate the involvement of TRAF1 in $A\beta_{1-42}$-induced apoptosis.

The dysfunction of the endoplasmic reticulum (ER) is involved in the pathogenesis of neurodegenerative diseases including AD[20]. Many conditions can lead to alteration of the protein folding status in the ER, resulting in a condition known as ER stress. Knowledge regarding induction of ER stress in AD remains rudimentary. It has been proposed that Aβ could be a potential trigger of ER stress in AD[21]. When the ER homeostasis cannot be restored, a pro-apoptotic response is induced. To tackle with ER stress, the unfolded protein response (UPR) is activated as an adaptive reaction to regulate the expression of hundreds of genes. Protein disulfide isomerases (PDIs) is induced under pathological conditions in the nervous system as a group of well-recognized UPR-target genes. PDIs are being explored as interesting therapeutic targets and biomarkers for multiple neurodegenerative diseases related to protein misfolding and ER stress. ERp57 is one of the main studied members of PDI family in the nervous system and could catalyze the disulfide bonds formation of glycoproteins through the physical association with the endoplasmic reticulum (ER) chaperones calnexin and calreticulin. ERp57 has been found to be markedly up-regulated in the temporal lobes from patients affected with Alzheimer's disease[22], which is believed to be correlated with the formation of neurofibrillary tangles. Another report identifies ERp57 as a pro-apoptotic regulator in models of Huntington's disease and AD[23]. It's interesting that ERp57, and another member of the PDI family, PDIA6, also known as ERp5, were observed with induction by Aβ in microglia[24]. In our study, microarray and PF-2D analysis showed that the expression levels of ERp57 and ERp5 were also increased in SH-SY5Y cells after $A\beta_{1-42}$ treatment. Thus, we hypothesize that $A\beta_{1-42}$ induces ER stress pathways involving ERp57 and ERp5, which may have relevance for neurodegenerative processes and neuronal death.

Cyclic AMP (cAMP) is a second messenger that regulates many diverse cellular functions, including gene transcription, cell migration, mitochondrial homeostasis, cell proliferation and cell death[25]. cAMP is synthesized by adenylyl cyclases (AC) and degraded by a single superfamily of hydrolases, the PDEs. Among the large PDE families, only PDE4, PDE7 and PDE8 are cAMP-specific. The imbalance of cAMP has been suggested to play a role in the etiology of AD[26]. Moreover, the alterations in expression of cAMP-specific PDEs mRNA was observed in AD brains[27]. Our data showed an increase in PDE8A and a decrease in PDE4C after $A\beta_{1-42}$ treatment. This observation suggests that there are possible different roles for PDE8A/PDE4C in $A\beta_{1-42}$ neurotoxicity.

Conclusion

These findings emphasize the potential role of Egr1, EIF5A, TRAF1, ERp5, ERp57, PDE8A and PDE4C in mediating Aβ-induced neuronal apoptosis. In the future, new experiments should be performed in order to delineate the relative contribution of these altered genes and protein in the neuropathological mechanism of AD, offering novel therapeutic targets for AD treatment.

Acknowledgements This work was supported by National Natural Science Funds of China (No. 81703831), the Budget Project of Shanghai Municipal Education Commission (No. 2014YSN05) and Program of Supporting Young Teachers in Shanghai College, China (No. ZZSZY15003).

Conflict of Interest Zhonghao Su declares that he has no conflict of interest. Zhuo Dong declares that he has no conflict of interest. Chunxia Guo declares that she has no conflict of interest. Ying Xu declares that she has no conflict of interest. Shuijin Shao declares that he has no conflict of interest. Zhenxia Qin declares that she has no conflict of interest.

Human and animals rights The article does not contain any studies with human and animal and this study was

performed following institutional and national guidelines.

Author contributions Z.S., Z.D., C.G., Y.X., S.S., and Z.Q. designed the experiments. Z.S. performed the experiments. Z.Q. and Z.S. analyzed the data. Z.S., S.S., and Z.Q. wrote the manuscript. Y.X. gave technical support. All authors reviewed the manuscript.

References

1. Hartley, D. M. *et al*. Protofibrillar intermediates of amyloid beta-protein induce acute electrophysiological changes and progressive neurotoxicity in cortical neurons. *J Neurosci* **19**, 8876-8884 (1999).
2. Mattson, M. P. *et al*. beta-Amyloid peptides destabilize calcium homeostasis and render human cortical neurons vulnerable to excitotoxicity. *J Neurosci* **12**, 376-389 (1992).
3. Qin, Z. *et al*. Mutated recombinant human glucagon-like peptide-1 protects SH-SY5Y cells from apoptosis induced by amyloid-beta peptide (1-42). *Neurosci Lett* **444**, 217-221 (2008).
4. Walsh, D. M. *et al*. Naturally secreted oligomers of amyloid beta protein potently inhibit hippocampal long-term potentiation in vivo. *Nature* **416**, 535-539 (2002).
5. Martinez, T. & Pascual, A. Gene expression profile in beta-amyloid-treated SH-SY5Y neuroblastoma cells. *Brain Res Bull* **72**, 225-231 (2007).
6. Heinitz, K., Beck, M. Schliebs, R. & Perez-Polo, J. R. Toxicity mediated by soluble oligomers of beta-amyloid (1-42) on cholinergic SN56.B5.G4 cells. *J Neurochem* **98**, 1930-1945 (2006).
7. Kim, J. R. *et al*. Identification of amyloid beta-peptide responsive genes by cDNA microarray technology: involvement of RTP801 in amyloid beta-peptide toxicity. *Exp Mol Med* **35**, 403-411 (2003).
8. Greenbaum, D., Colangelo, C., Williams, K. & Gerstein, M. Comparing protein abundance and mRNA expression levels on a genomic scale. *Genome Biol* **4**, 117 (2003).
9. Paulson, L. *et al*. Comparative genome- and proteome analysis of cerebral cortex from MK-801-treated rats. *J Neurosci Res* **71**, 526-533 (2003).
10. Barre, O. & Solioz, M. Improved protocol for chromatofocusing on the ProteomeLab PF2D. *Proteomics* **6**, 5096-5098 (2006).
11. Qin, Z. X., Zhu, H. Y. & Hu, Y. H. Effects of lysophosphatidylcholine on beta-amyloid-induced neuronal apoptosis. *Acta Pharmacol Sin* **30**, 388-395 (2009).
12. Honore, B., Ostergaard, M. & Vorum, H. Functional genomics studied by proteomics. *Bioessays* **26**, 901-915 (2004).
13. Lu, Y. *et al*. Early growth response 1 (Egr-1) regulates phosphorylation of microtubule-associated protein tau in mammalian brain. *J Biol Chem* **286**, 20569-20581.
14. Saini, P., Eyler, D. E., Green, R. & Dever, T. E. Hypusine-containing protein eIF5A promotes translation elongation. *Nature* **459**, 118-121 (2009).
15. Jansson, B. P., Malandrin, L. & Johansson, H. E. Cell cycle arrest in archaea by the hypusination inhibitor N (1)-guanyl-1,7-diaminoheptane. *J Bacteriol* **182**, 1158-1161 (2000).
16. Sun, Z. *et al*. Apoptosis induction by eIF5A1 involves activation of the intrinsic mitochondrial pathway. *J Cell Physiol* **223**, 798-809 (2010).
17. Lee, S. Y. & Choi, Y. TRAF1 and its biological functions. *Adv Exp Med Biol* **597**, 25-31 (2007).
18. Jang, H. D. *et al*. Caspase-cleaved TRAF1 negatively regulates the antiapoptotic signals of TRAF2 during TNF-induced cell death. *Biochem Biophys Res Commun* **281**, 499-505 (2001).
19. Wang, C. Y. *et al*. NF-kappaB antiapoptosis: induction of TRAF1 and TRAF2 and c-IAP1 and c-IAP2 to suppress caspase-8 activation. *Science* **281**, 1680-1683 (1998).
20. Hetz, C. & Mollereau, B. Disturbance of endoplasmic reticulum proteostasis in neurodegenerative diseases. *Nat Rev Neurosci* **15**, 233-249 (2014).
21. Zhang, L. *et al*. Tetrahydroxystilbene glucoside antagonizes age-related alpha-synuclein overexpression in the hippocampus of APP transgenic mouse model of Alzheimer's disease. *Restor Neurol Neurosci* **31**, 41-52 (2013).
22. Lee, J. H. *et al*. Induction of the unfolded protein response and cell death pathway in Alzheimer's disease, but not in aged Tg2576 mice. *Exp Mol Med* **42**, 386-394 (2010).
23. Hoffstrom, B. G. *et al*. Inhibitors of protein disulfide isomerase suppress apoptosis induced by misfolded proteins. *Nat Chem Biol* **6**, 900-906 (2010).
24. Yoo, Y. *et al*. Amyloid-beta-activated human microglial cells through ER-resident proteins. *J Proteome Res* **14**, 214-223 (2015).
25. Lefkimmiatis, K. & Zaccolo, M. cAMP signaling in subcellular compartments. *Pharmacol Ther* **143**, 295-304 (2014).
26. Bollen, E. & Prickaerts, J. Phosphodiesterases in neurodegenerative disorders. *IUBMB Life* **64**, 965-970 (2012).
27. Perez-Torres, S. *et al*. Alterations on phosphodiesterase type 7 and 8 isozyme mRNA expression in Alzheimer's disease brains examined by in situ hybridization. *Exp Neurol* **182**, 322-334 (2003).